



Charcoal and Use of Green Binder for Use in Carbon Anodes in the Aluminium Industry

Camilla Sommerseth, Ove Darell, Bjarte Øye, Anne Støre, and Stein Rørvik

Abstract

Carbon anodes for aluminium production are produced from calcined petroleum coke (CPC), recycled anode butts and coal tar pitch (CTP). The CO₂ produced during anode consumption contributes to a substantial amount of the CO₂ footprint of this industrial process. Charcoal from wood has been suggested to partly replace coke in anodes but high porosity, low electrical resistivity and high ash content contributes negatively to final anode properties. In this work, charcoal from Siberian larch and spruce was produced by heat treatment to 800, 1200 and 1400 °C and acid-washed with H₂SO₄. Acid-washing resulted in reduced metal impurity and the porosity decreased with increasing heat treatment. Pilot anodes were made from CTP, CPC with some additions of spruce and larch charcoal. Another set of pilot anodes were produced using a green binder. Compared to reference anodes, the CO₂ reactivity of anodes containing larch was less affected compared to anodes containing spruce. The green binder was found to be highly detrimental for the anodes' CO₂ reactivity properties. Electrochemical consumption increased for anodes containing both green binder, larch and spruce compared to the reference anode.

Keywords

Charcoal production • Spruce • Siberian larch • Heat treatment • Acid-washing

Introduction

Most countries in the world agreed through the Paris agreement to take measures in order to reduce CO₂ emissions. Replacing fossil fuel-based carbon in process industry

by biocarbon or charcoal is one possible option. Carbon anodes for aluminium production are produced from calcined petroleum coke (CPC), coal tar pitch (CTP) and recycled anode butts. By introducing charcoal produced from wood, the global warming footprint of the aluminium industry may be reduced. Monsen et al. [1] investigated using charcoal from maple, spruce and an Indonesian source. They found that charcoal could only be used as fines due to the high porosity of the carbon structure. The density of anodes containing charcoal was reduced and CO₂ reactivity increased. The conclusion was that they did not recommend using charcoal in anodes. Recent work [2, 3] has shown that acid-washing and further heat treatment of the charcoal may reduce the undesirable effects of high porosity, high ash content as some of these elements are known to give increased air and CO₂ reactivity.

In this work, spruce and Siberian larch (from now on denoted as larch only) were studied. Spruce was chosen in order to investigate if it was possible to improve the negative effects observed in [1] by further heat treatment and acid-washing by H₂SO₄ of the charcoal and larch was chosen due to its abundance and high density. A green binder was also investigated to replace coal tar pitch and, in that way, reducing the fossil CO₂ footprint of anode production.

Materials and Methods

Charcoal Production

Wood from spruce and larch was chopped into pieces of 7 × 5 × 5 cm³. The wood pieces were placed in a steel box, covered with packing coke and calcined to 800 °C in a chamber furnace. Some of the wood was then calcined further to 1200 or 1400 °C. The heating rate was 300 °C/h with a hold time of 5 h. The charcoal was either washed in 0.1 or 1.0 M sulfuric acid, H₂SO₄. H₂SO₄ was chosen due to the positive effect sulfur has on CO₂ reactivity of anodes. A magnetic stirrer was used during the acid-washing and the

C. Sommerseth (✉) · O. Darell · B. Øye · A. Støre · S. Rørvik
SINTEF Industry, 4760 Torgarden, 7465 Trondheim, Norway
e-mail: camilla.sommerseth@sintef.no

charcoal pieces was left in the acid solution for 10–12 h at 67 °C before being washed, then rinsed in fresh water for one hour and dried at 120 °C. After the acid-washing with sulfuric acid, a white precipitate was observed on the charcoal. This was removed by soaking the charcoal in 7 % acetic acid for 10–12 h at 67 °C and then rinsed in water for 2–3 h before being dried at 120 °C. Table 1 shows a summary of the charcoal production including the abbreviated names for each charcoal type.

Anode Production

Table 2 shows an overview of the aggregate composition of the produced anodes. The coke aggregate was produced with particles smaller than 2 mm to ensure homogeneous samples during small-scale characterization and electrolysis testing. The anodes contained 30 wt% fines less than 0.125 mm. Charcoal was only added to the fines. The 0.125–1 and 1–2 mm coke particles each made up 35 wt% of the coke aggregate. Pitch, coke particles and fines were dry mixed in a beaker and heated to 180 °C. The pitch, coke and fines were further mixed on a heating plate before being compressed in a mould at 180 °C. The mould was placed in the heating cabinet at 180 °C for another 30 min. The mixture was then hot-pressed at 30 kN. Anodes containing green binder was produced by placing the binder, coke particles and fines in separate containers in a heating cabinet at 50 °C before being mixed together in a beaker. The mixture was poured into a compression mould and placed in the heating cabinet at 50 °C for 30 min before being hot-pressed at 30 kN. All anodes were baked to 1260 °C with a hold time of two hours and a heating and cooling rate of 80 °C/h. The green binder used for anode making had a consistence like syrup.

Charcoal Characterization

High Resolution Inductive coupled plasma mass spectrometry (ICP-MS) was used to investigate the elemental impurities in the charcoal samples before and after acid-washing. Samples of charcoal (<500 mg) were dissolved into 80 mL of 50 % HNO₃ in an UltraClave and the solutions were then analysed in the ICP-MS ELEMENT 2 from Thermo Electronics.

A micro X-ray computed tomography (μ CT) was used as a non-destructive test to investigate the interior of the anode samples using a Nikon XT H225 ST instrument (cone beam volume CT). A tungsten reflection target was used, with an acceleration voltage of 135 kV and a current of 200 μ A. The radiation was not filtered. The imaging was done with an integration time of 1 s, amplification of 18 dB, with 6283 projections per 360°. The distance from source to sample was 156.72 mm, distance from source to detector was 1127.5 mm, resulting in a voxel size of (27.8 μ m)³. The images were exported as 16-bit TIFF and processed in the public domain software ImageJ.

Raman spectroscopy was used to determine the degree of graphitization of petroleum coke and charcoal. The spectra were recorded at room temperature using a Renishaw InVia Raman spectrometer. The excitation light source was a 532 nm laser. The laser beam was focused using a 50x objective. Spectra were recorded at eight different positions on each sample to investigate the spatial variations. The samples were placed on a glass slide and spectra were recorded in the range 850–2000 cm⁻¹. Spectra were recorded as an average of 10 individual spectra with 10 s integration time. The laser power was reduced to 1 % to ensure no sample degradation during the acquisition. The curve fitting to obtain quantitative parameters was based on the work by Li, Hayashi and Li [4], however, some modifications were made to fit the present work. The charcoal in the

Table 1 Charcoal production and acid-washing with sulfuric acid

Wood type	Heat treatment, °C	Acid-washing, H ₂ SO ₄ , M	Charcoal short name
Spruce	800	0.1	S800-0.1
Spruce	1200	0.1	S1200-0.1
Spruce	1400	0.1	S1400-0.1
Spruce	800	1.0	S800-1.0
Spruce	1200	1.0	S1200-1.0
Spruce	1400	1.0	S1400-1.0
Larch	800	0.1	L800-0.1
Larch	1200	0.1	L1200-0.1
Larch	1400	0.1	L1400-0.1
Larch	800	1.0	L800-1.0
Larch	1200	1.0	L1200-1.0
Larch	1400	1.0	L1400-1.0

Table 2 Summary of the anodes produced, all numbers in wt%

Anode name	Charcoal type	Charcoal in fines	CPC fines	Coke 0.125–1 mm	Coke 1–2 mm	Binder type	Binder amount
Green ref-1			30	35	35	Green	16.7
Green ref-2			30	35	35	Green	23.1
Pitch ref-1			30	35	35	CTP	13.0
Pitch ref-2			30	35	35	CTP	13.0
Pitch ref-3			30	35	35	CTP	16.7
Pitch ref-4			30	35	35	CTP	23.1
SG800-1.0-5 %	S800-1.0	5	25	35	35	Green	16.7
SG800-1.0-10 %	S800-1.0	10	20	35	35	Green	16.7
SG800-1.0-15 %	S800-1.0	15	15	35	35	Green	16.7
SG1400-1.0-5 %	S1400-1.0	5	25	35	35	Green	16.7
SG1400-1.0-10 %	S1400-1.0	10	20	35	35	Green	16.7
SG1400-1.0-15 %-1	S1400-1.0	15	15	35	35	Green	16.7
SG1400-1.0-15 %-2	S1400-1.0	15	15	35	35	Green	23.1
SP800-1.0-5 %	S800-1.0	5	25	35	35	CTP	13.0
SP800-1.0-10 %	S800-1.0	10	20	35	35	CTP	13.0
SP800-1.0-15 %	S800-1.0	15	15	35	35	CTP	13.0
SP1400-1.0-5 %	S1400-1.0	5	25	35	35	CTP	13.0
SP1400-1.0-10 %	S1400-1.0	10	20	35	35	CTP	13.0
SP1400-1.0-15 %-1	S1400-1.0	15	15	35	35	CTP	13.0
SP1400-1.0-15 %-2	S1400-1.0	15	15	35	35	CTP	17.4
SP1400-1.0-15 %-3	S1400-1.0	15	15	35	35	CTP	23.1
SP1400-0.1-15%	S1400-1.0	15	15	35	35	CTP	13.0
LG800-1.0-5 %	L800-1.0	5	25	35	35	Green	16.7
LP800-1.0-5 %	L800-1.0	5	25	35	35	CTP	13.0
LP800-1.0-10 %	L800-1.0	10	20	35	35	CTP	13.0
LP800-1.0-15 %	L800-1.0	15	15	35	35	CTP	13.0
LP1400-1.0-15 %-1	L1400-1.0	15	15	35	35	CTP	18.1
LP1400-1.0-15 %-2	L1400-1.0	15	15	35	35	CTP	13.0
LP1400-0.1-5 %	L1400-0.1	5	25	35	35	CTP	13.0
LP1400-0.1-10 %	L1400-0.1	10	20	35	35	CTP	13.0
LP1400-0.1-15 %	L1400-0.1	15	15	35	35	CTP	13.0

present work was heat treated to a substantially higher temperature compared to the reference work, i.e. 800, 1200 and 1400 °C vs. 500, 600, 700, 800 and 900 °C. The Raman spectra were curve fitted using five band positions including one additional graphite band where a wider full width half maximum (FWHM) value was allowed, named G_{wide} . This was done to take into consideration that the sample is not homogeneous, but a mixture of amorphous and more graphitic structures. The band fitting was greatly improved by introducing G_{wide} . Some of the band positions was slightly shifted compared to the reference work, and the bands G_L , G_R , V_R , S_R and R were excluded from the present work

since these carbonaceous species were considered less likely to be present at these high temperature treatments. Table 3 gives a summary of the Raman bands used for curve fitting. To improve the curve fit, some tolerance was allowed by introducing minimum and maximum values for the band positions, the FWHM and the height of the bands/peaks.

Specific surface area of the charcoal samples was determined by measuring gas adsorption according to the Brunauer Emmet and Teller (BET) technique and ISO 9277:2010 [5]. A Micrometrics TriStar 3000 Surface Area and Porosity Analyzer instrument was used. Pore volume was determined by Barrett, Joyner and Halenda

Table 3 Positions of Raman bands used for curve fitting

Band name	Minimum band position, cm^{-1}	Maximum band position, cm^{-1}	Minimum FWHM, cm^{-1}	Maximum FWHM, cm^{-1}	Minimum band height	Maximum band height
S _L	1230	1255	20	100	20	1000
S	1170	1190	20	100	20	2000
D	1300	1350	20	200	20	10,000
V _L	1450	1500	20	200	20	5000
G	1590	1600	20	70	20	10,000
G _{wide}	1590	1600	20	200	20	10,000

(BJH) desorption. In the tests, 0.1–1.0 g charcoal sample, degassed at 250 °C in vacuum overnight, was used. A filler rod was used in the sample glasses to reduce measurement errors. The adsorption and desorption isotherms were recorded with 40 points for each isotherm.

Scanning electron microscope (SEM) was used to investigate the effect of heat treatment on the pore structure. A small amount of charcoal fines was put on a 15 mm sample holder using a double-adhesive carbon tape. The acceleration voltage was 10 kV with an emission current of 125 μA . Images were captured at 100x and 500x magnification.

Anode Characterization

The density (g/cm^3) of the anodes was determined according to ISO 5017:2013 [6], immersing dry weighed anode samples into water.

The specific electrical resistivity (SER) was measured on the sample surface using a Wenner array with four spring-loaded pins. The four pins were spaced at 10 mm distance. A constant current of 1 A was applied to the outermost pins and SER was calculated from the measured voltage drop across the innermost pins.

The CO₂ reactivity of the anode samples were investigated using an in-house technique based on ISO 12988-1:2000 [7]. Two 10 mm diameter samples of each anode were core drilled, weighed and placed in a closed furnace with argon atmosphere (5.0, flow: 20 NL/h) and heated to 960 °C. The samples were kept under argon atmosphere for another hour to assure even temperature in the furnace. Then the gas was switched to CO₂ (5.2, flow: 20 NL/h) with a hold time of 2.5 h. After CO₂ exposure, the samples were cooled down under argon atmosphere, weighed and brushed to remove dust and loose material before being weighed again.

Electrochemical Consumption of the Anodes

The electrochemical consumption of the anodes was investigated at 1.0 A/cm² for 45 min using 9.6 mm diameter

anodes immersed 1 cm in industrial bath with 11.1 wt% AlF₃ and 3.26 wt% Al₂O₃.

Results and Discussion

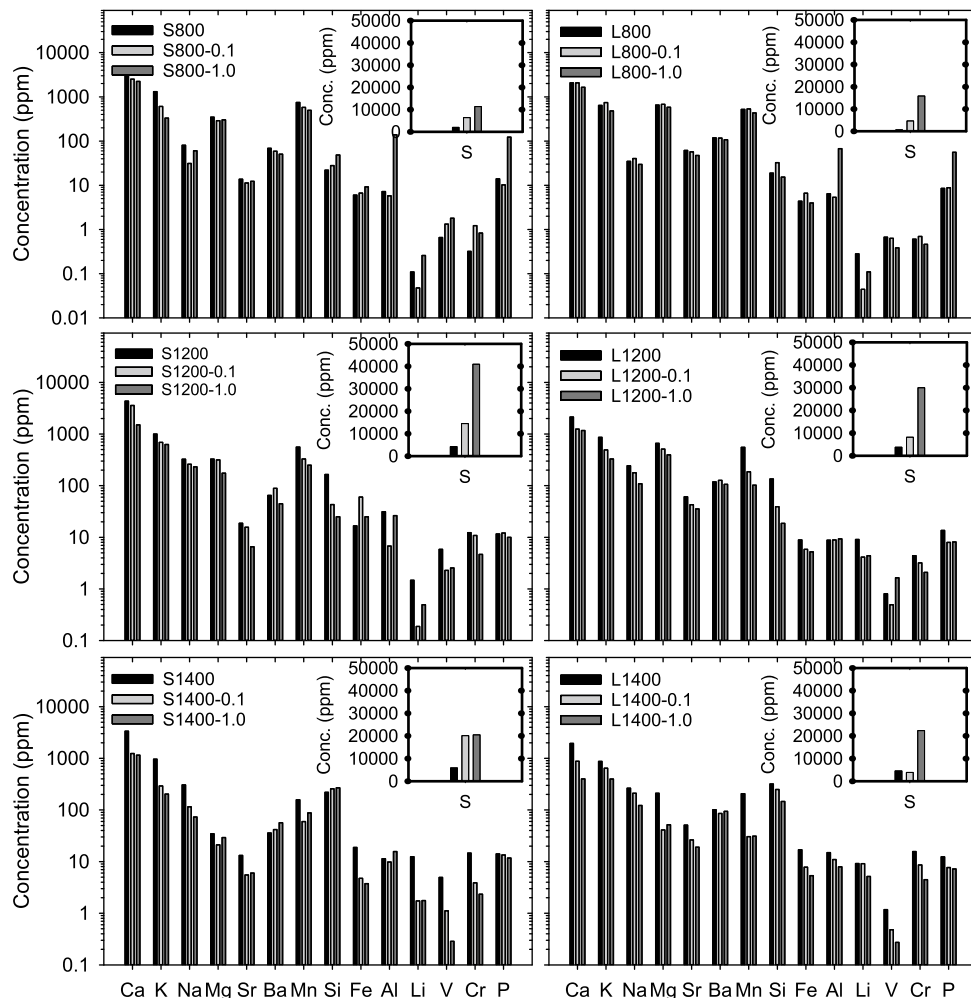
Charcoal Characterization

ICP-MS was used to compare the effect of acid-washing of the charcoal. Figure 1 shows the elemental analysis results. The concentration of most elements decreased with acid-washing and more for the charcoals heat treated at the highest temperatures. For larch, the effect of acid-washing with 1.0 M H₂SO₄ is more pronounced than for spruce, probably due to larch having a more open pore structure. The sulfur content increases after acid-washing, as was expected and intended to investigate the effect of sulfur on the CO₂ reactivity. The charcoals are higher in alkali and earth alkali elements such as Na and Ca compared to CPC, but lower in metallic content such as V and Fe. Vanadium is known to be a strong catalyst for air reactivity, so less V can be favourable in anodes [8].

Figure 2 shows μCT and SEM images of spruce (top) and larch (bottom) calcined at 1400 °C. The annual growth rings are very visible for the spruce charcoal, while the larch looks more porous. The heat treatment alone did not collapse the pore structure of the charcoals, similar to what was found in [1]. The charcoal was then crushed to fines of <0.125 mm particles and examined in SEM as shown to the right in Fig. 2, showing that most of the pore structure is broken. This is in accordance with what Hussein et al. found [3]. Hence, heat treatment is not sufficient to break the entire pore structure of the charcoal, regardless of the heat treatment range.

Figure 3 shows the results from the Raman spectroscopy of the charcoal and the CPC. According to Li, Hayashi and Li [4], G is the graphite band and D is the defect band. Furthermore, the D band can represent medium-to-large sized aromatic ring systems with 6 or more rings. The S band represents sp²-sp³ carbonaceous structures, aromatic ethers, C_{aromatic}-C_{alkyl} bonds, C-C bonds on hydroaromatic

Fig. 1 Elemental analysis of the charcoals, non-acid-washed and acid-washed to 0.1 and 1.0 M H_2SO_4 . Note that the scale is logarithmic. The sulfur concentration is included, using a linear scale



rings and C-H bonds on aromatic rings. Finally, V_L is attributed to methylene or methyl, semi-circle breathing of aromatic rings and amorphous carbon structures. As previously mentioned, G_{wide} was included in the present work to take into consideration the presence of amorphous graphite. The ratio between $D/(G + G_{\text{wide}})$ in Fig. 3, can be used to investigate the structural ordering of carbon during heat treatment. In general, a decreasing trend is seen with increasing heat treatment of the charcoal. However, within the uncertainty, the degree of graphitization is similar between spruce and larch heat treated to 1200 and 1400 °C, but much less structured than CPC. The increasing trend for D/V_L with heat treatment represents an increasing size of the aromatic clusters. The decreasing trend for $S/(G + G_{\text{wide}})$ and the bandwidth D also represents increasing graphitic ordering and ordering of the hydroaromatic rings.

Figure 4 shows pore volume as a function of pore diameter for spruce (top) and larch (middle) and BET surface area for the charcoals and CPC. BET surface area and pore volumes are much higher for the charcoals compared to CPC, regardless of the calcination temperature. Spruce has more pores or longer pores than larch. For larch it is evident that increasing heat treatment reduces the pore volume and the BET surface area. This trend is not that evident for spruce, as the temperature increase from 1200 to 1400 °C increased the BET surface area. The high porosity of the charcoals makes charcoal rather undesirable for use in anodes, similar to what Monsen et al. [1] found where they advised against using charcoal. However, Hussein et al. [2] suggested that adjustments to the anode recipe, for example by increasing the pitch content could mitigate some of the negative effects of charcoal additions.

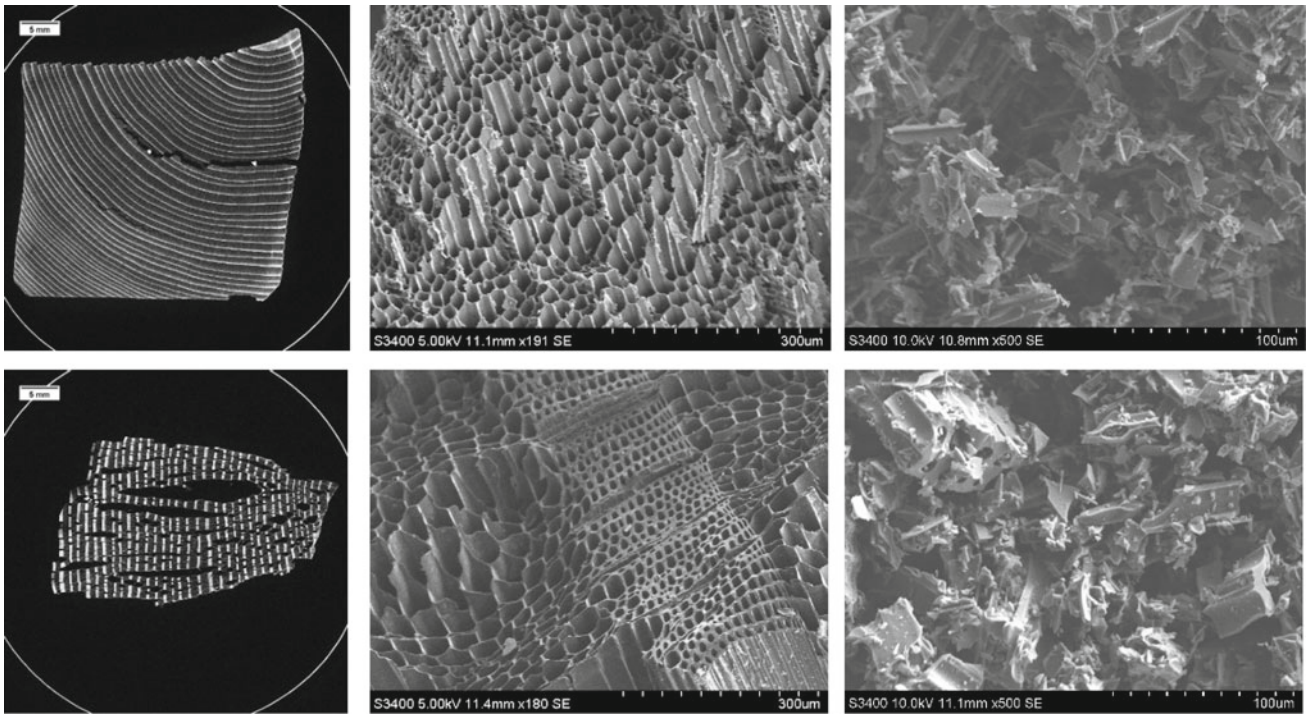
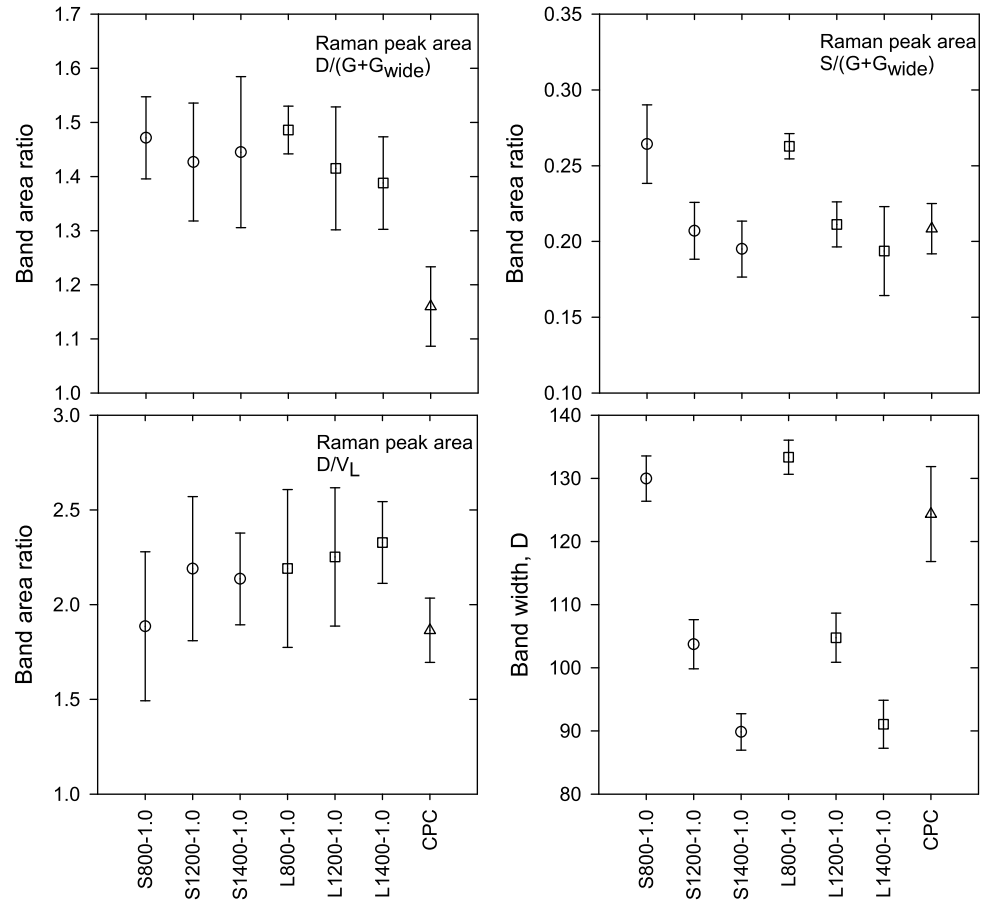


Fig. 2 Top from left to right: μ CT images of spruce, SEM image of the same spruce and SEM image of crushed spruce. Bottom left to right: μ CT images of spruce, SEM image of the same spruce and SEM image of crushed spruce. The charcoals were calcined to 1400 °C

Fig. 3 Raman results after curve fitting. Top left: $D/(G + G_{wide})$ band area ratio. Top right: $S/(G + G_{wide})$ band area ratio. Bottom left: D/V_L and bottom right: D band width. The results are a function of charcoal/carbon type



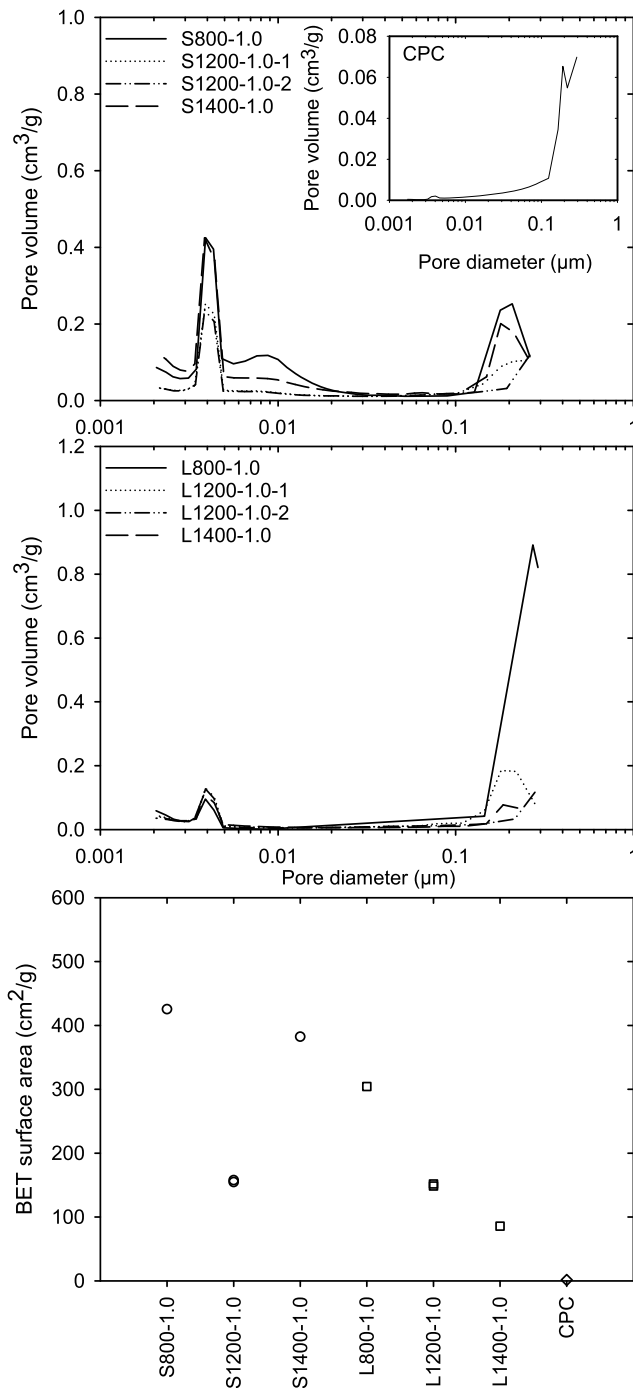


Fig. 4 Pore volume for charcoal from spruce (top), larch (middle), including an insert of CPC with corresponding BET surface area (bottom)

Anode Characterization

The anodes were characterized using traditional techniques: CO_2 reactivity, SER and density. Table 4 shows that green

binder was highly detrimental to the CO_2 reactivity for anodes containing charcoal or CPC only. The higher green binder content for Green-ref 2 was so detrimental that the entire samples burned during the CO_2 reactivity test, leaving only dust behind. Hence, this green binder cannot be used in anodes. The residue percentage varies for the four reference anodes containing CTP and CPC (Pitch ref-1-4), most likely due to production variations in the laboratory, and for Pitch ref-4 the higher pitch content. The specific electrical resistivity and density do not reflect differences between the four reference anodes (Pitch ref-1-4, Fig. 5). Charcoal from spruce increases the CO_2 reactivity in accordance with the findings of Monsen, Ratvik and Lossius [1]. However, increased heat treatment of spruce charcoal reduced the CO_2 reactivity. Green binder was not as detrimental to the anodes' reactivity when larch charcoal was used. For LP800-1.0-5, LP800-1.0-10 and LP800-1.0-15 %, the CO_2 reactivity decreased with increasing larch charcoal content. Increased calcination from 800 to 1400 °C of the larch charcoal reduced the CO_2 reactivity for the anodes. Anodes containing as much as 15 % larch had comparable CO_2 residue (W-RCR) to the Pitch-ref anodes. When comparing the effect of the sulfuric acid, it is evident that increased acid strength decreases the CO_2 reactivity. The higher pitch content of anode LP1400-1.0-15 %-1 (18.1 % pitch) compared to LP1400-1.0-15 %-2 (13.0 % pitch) appear to have a positive effect on the CO_2 reactivity, similar to reference [2]. It is known that sulfur in anodes decreases the CO_2 reactivity [9], and it appears that sulfur from sulfuric acid also has this effect. Anodes containing spruce are dusting (W-RCD) much more than anodes containing larch, however the loss (W-RCL) during reaction with CO_2 is similar. When comparing LP1400-1.0-15 %-2 to LP1400-0.1-15 %, the charcoal that was acid-washed at 1.0 M shows a significantly reduced CO_2 reactivity compared to the charcoal acid-washed at 0.1 M H_2SO_4 , showing that sulfur from H_2SO_4 reduces the CO_2 reactivity. In Norway where SO_2 scrubbers are installed at all aluminium plants, increased sulfur content is not an environmental problem.

Figure 5 shows that SER and density of the produced anodes are closely correlated. Green binder is found to be detrimental to the density and SER compared to anodes produced with CTP. Again, larch shows better trends in terms of SER and density when compared to equivalent anodes containing spruce. For anodes containing spruce it is observed a strong negative correlation to the anode's properties with increased spruce content. This correlation is not as apparent for anodes containing larch. The density of the anodes appears to be little affected by increased heat treatment of the charcoal. It is to be noted that SER is higher and the density lower than industrial standard or the Pitch ref-1-4

Table 4 CO₂ reactivity for the anodes given as average of two repeat samples and one standard deviation

Anode	Binder, wt%	Residue W-RCR, %	Std. dev., ±	Dust W-RCD, %	Std. dev., ±	Loss W-RCL, %	Std. dev., ±
Green ref-1	16.7	29.4	7.3	63.9	7.2	6.8	0.1
Green ref-2	23.1	0	0	92.1	0.9	7.9	0.9
Pitch ref-1	13.0	90.1	2.3	4.5	1.6	5.3	0.7
Pitch ref-2	13.0	78.8	4.8	11.4	3.7	9.8	1.2
Pitch ref-3	16.7	94.8	0.8	0.6	0	4.6	0.8
Pitch ref-4	23.1	78.7	5.3	15.5	3.8	5.8	1.5
SG800-1.0-5 %	16.7	19.2	5.1	69.3	4.5	11.5	0.7
SG800-1.0-10 %	16.7	7.1	10.0	77.6	9.0	15.4	1.0
SG800-1.0-15 %	16.7	0.0	0.0	75.9	4.5	24.1	4.5
SG1400-1.0-5 %	16.7	16.1	14.5	72.7	13.7	11.2	0.8
SG1400-1.0-10 %	16.7	0.0	0.0	85.0	0.1	15.0	0.1
SP800-1.0-5 %	13.0	75.0	2.9	14.1	3.0	10.8	0.1
SP800-1.0-10 %	13.0	47.9	10.2	35.1	10.3	17.0	0.1
SP800-1.0-15 %	13.0	40.5	1.7	41.8	0.5	17.8	1.2
SP1400-1.0-5 %	13.0	86.6	1.9	4.0	1.0	9.4	1.0
SP1400-1.0-10 %	13.0	81.6	4.4	6.1	3.8	12.3	0.6
SP1400-1.0-15 %-1	13.0	66.8	7.6	17.5	5.4	15.7	2.1
LG800-1.0-5 %	16.7	64.7	5.4	26.0	5.2	9.2	0.3
LP800-1.0-5 %	13.0	74.8	2.7	13.9	2.5	11.3	0.2
LP800-1.0-10 %	13.0	76.2	2.2	9.1	0.7	14.8	1.6
LP800-1.0-15 %	13.0	79.4	1.2	5.1	1.5	15.5	0.3
LP1400-1.0-15 %-1	18.1	88.8	0.1	0.7	0.0	10.5	0.0
LP1400-1.0-15 %-2	13.0	85.4	4.1	2.8	1.5	11.7	2.6
LP1400-0.1-5 %	13.0	83.1	3.3	6.6	3.2	10.2	0.1
LP1400-0.1-10 %	13.0	64.9	2.5	22.2	1.1	12.9	1.4
LP1400-0.1-15 %	13.0	62.4	2.9	22.5	1.2	15.1	1.7

anodes, and the measurements for one industrial prebake standard is included to underline this. Hence, laboratory anodes are not directly comparable to industrial standards.

Electrochemical Consumption

A selection of anodes was chosen to investigate the effect of increased CO₂ reactivity and lower density of anodes containing green binder and spruce and larch charcoal to the electrochemical consumption compared the Pitch ref-3 reference. The anodes were electrolyzed at 1.0 A/cm² for 45 min with two repeats for all anodes. The results of the

testing are shown in Fig. 6. Pitch ref-3 shows less electrochemical consumption than all the other anodes, and the standard deviation is also very low indicating a homogeneous, reproducible sample creating very little dust and with limited CO₂ reactivity. Green ref-1 shows the highest electrochemical consumption and has the largest standard deviation. This is not surprising since the CO₂ reactivity test showed that this anode nearly fell apart and created a lot of dust. The anodes containing spruce and larch charcoal are all relatively similar, with LP1400-1.0-15 %-1 showing slightly lower electrochemical consumption than the other samples. In general, the electrochemical consumption results are in fair agreement with the CO₂ reactivity tests for these samples.

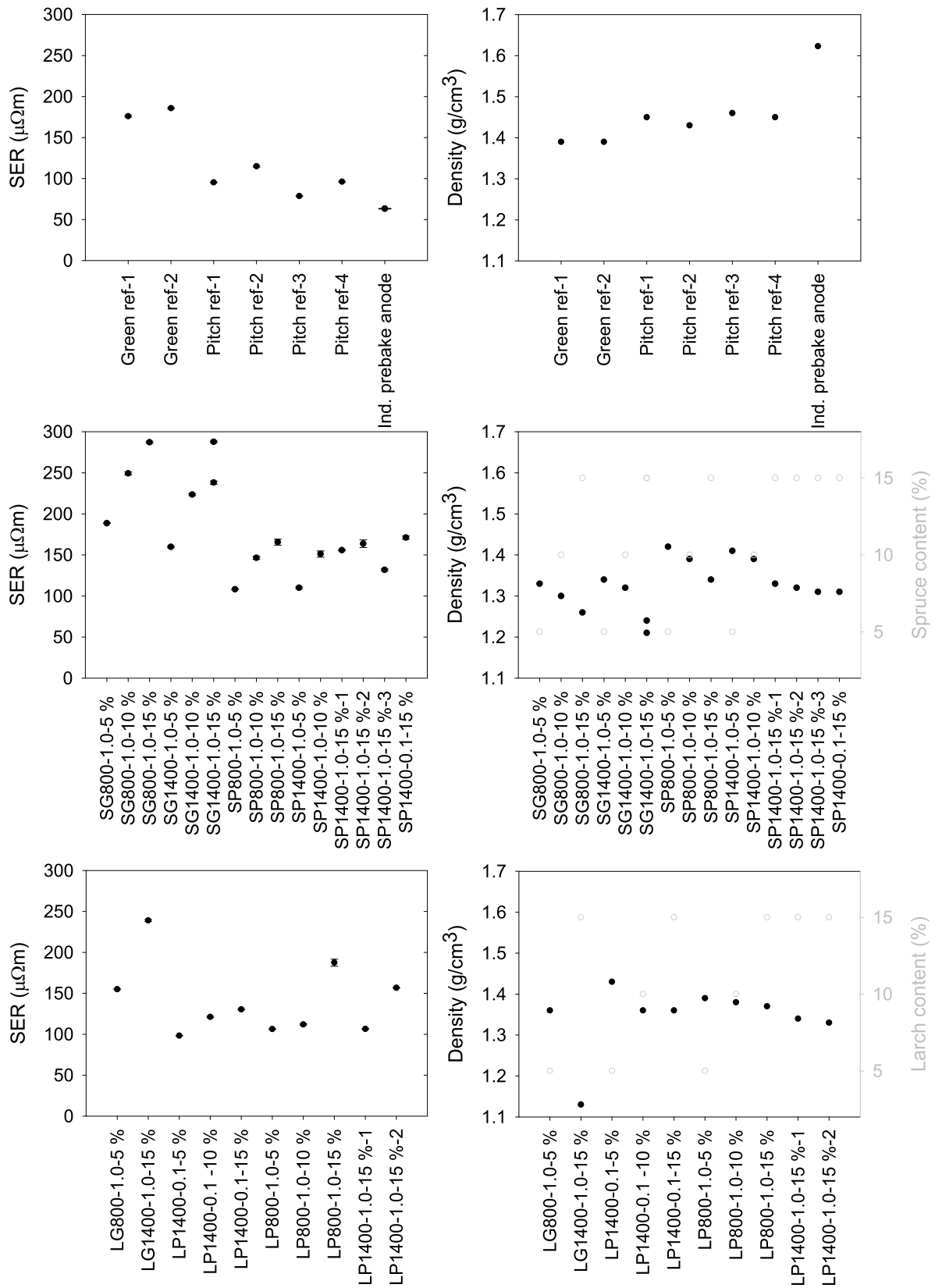


Fig. 5 Specific electrical reactivity with one standard deviation (left) and density (right) for the anodes. Open circles indicate the charcoal content in the anodes (right axis)

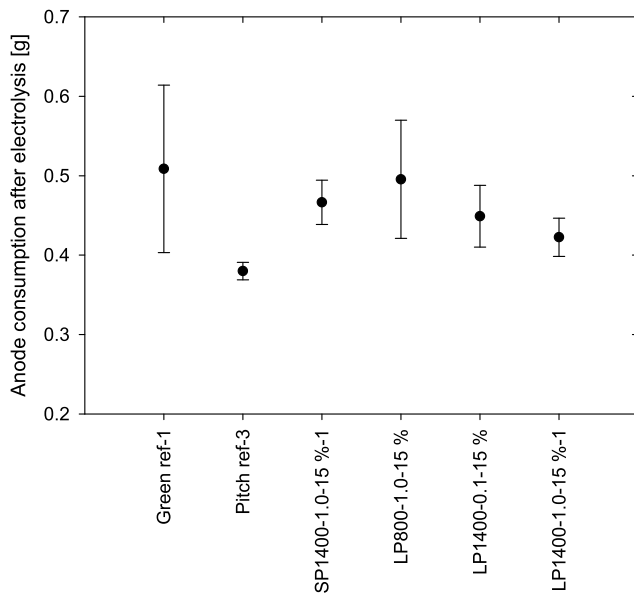


Fig. 6 Consumption of a selection of anodes after electrolysis

Conclusions

The effect of additions of spruce and Siberian larch charcoal, and the use of a green binder, were investigated when added to anodes for aluminium production. The laboratory produced anodes did not reach industrial standards regarding density and SER, however, all results show a deterioration of anode quality with additions of untraditional anode raw materials. The tested green binder was detrimental to anode quality and cannot be used in carbon anodes. Siberian larch showed better results regarding CO_2 reactivity, electrochemical consumption and BET surface area compared to spruce. The heat treatment did reduce the BET surface area but did not become comparable to CPC. Acid-washing with sulfuric acid reduced the elemental impurities of the

charcoal. However, the alkali and alkaline earth elements are very high in both wood charcoals making them challenging for use in carbon anodes.

Acknowledgements The Research Council of Norway is acknowledged for the support to NTNU NanoLab through the Norwegian Micro- and Nano-Fabrication Facility, NorFab, project number 245963/F50. NTNU NanoLab was used for Raman spectroscopy. Arne Røyset at SINTEF is acknowledged for performing Raman spectroscopy, curve-fitting and contributing to the discussions regarding the results.

References

1. Monsen BE, Ratvik AP, Lossius LP (2010) Charcoal in Anodes for Aluminium Production. *Light Metals* 2010:929–933
2. Hussein A, Fafard M, Ziegler D, Alamdari H (2017) Effects of Charcoal Addition on the Properties of Carbon Anodes. *Metals* 98:3. <https://doi.org/10.3390/met7030098>
3. Hussein A, Larachi F, Ziegler D, Alamdari H (2016) Effects of heat treatment and acid washing on properties and reactivity of charcoal. *Biomass and Bioenergy* 90:101–113. <https://doi.org/10.1016/j.biombioe.2016.03.041>
4. Li X, Hayashi J-i, Li C-Z (2006) FT-Raman spectroscopic study of the evolution of char structure during the pyrolysis of a Victorian brown coal. *Fuel* 85 (12–13):1700–1707. <https://doi.org/10.1016/j.fuel.2006.03.008>
5. Standardization IOF (2010) ISO 9277:2010. Determination of the specific surface area of solids by gas adsorption - BET method. International Organization for Standardization
6. Standardization IOF (2013) ISO 5017:2013. Dense shaped refractory products – Determination of bulk density, apparent porosity and true porosity. International Organization for Standardization
7. Standardization IOF (2000) ISO 12988-1:2000. Carbonaceous materials used in the production of aluminium - Baked anodes - Determination of the reactivity to carbon dioxide - Part 1: Loss in mass method. International Organization for Standardization
8. Tran KN, Berkovich AJ, Tomsett A, Bhatia SK (2009) Influence of Sulfur and Metal Microconstituents on the Reactivity of Carbon Anodes. *Energy & Fuels* 23 (4):1909–1924. <https://doi.org/10.1021/ef8009519>
9. Dreyer C, Samanos B, Vogt F (1996) Coke calcination levels and aluminium anode quality. *Light Metals* 1996:535–542